

Dispersion compensation for proximal scanning rigid OCT endoscopes

E. Lanke^a, M. Schumacher^a, P. Koch^a, F. König^b, D. Daniltchenko^b, D. Schnorr^b, G. Hüttmann^a

^aMedizinisches Laserzentrum Lübeck, Germany

^bKlinik für Urologie der Charité Berlin, Germany

ABSTRACT

Combining endoscopy with optical coherence tomography (OCT) can improve the diagnosis in minimal invasive procedures. Up to now OCT probes were constructed using rotating or moving single-mode fibers or micro scanners at the tip of the probe. We describe an endoscopic OCT system which uses a specially designed rigid endoscope with an extracorporeal scanner to create OCT images with 15 μm resolution. The OCT endoscope was constructed using a 270 mm gradient index lens with a diameter of 3 mm. Dispersion of the endoscope was compensated in the OCT interferometer by an all fiber approach. The system is now being tested for detecting malignancies in the urinary bladder.

Keywords: OCT, dispersion, endoscope, gradient index lens, fiber bundle, urology, urinary bladder, diagnosis

1. INTRODUCTION

Optical coherence tomography (OCT) is suitable for analyzing tissue layers up to a depth of 2 mm¹. A combination of OCT with endoscopy is needed to measure interior surfaces like bladder wall, esophagus or vessel walls. Several OCT systems for endoscopic use were described^{2,6,7,8} with a scanning mechanism placed at the intracorporeal end of a single-mode fiber. However this approach has several disadvantages. Miniaturization is difficult and the device has to withstand sterilization. A different way to obtain OCT images from inside the body is to use a rigid or flexible endoscope to transfer images outside the body, where it can be scanned by an OCT system. Endoscopic OCT^{9,10} with an extracorporeal scanner offers several advantages over a system with an intracorporeal scanner. It does not rely on specially designed miniature scanning devices and can easily combine OCT with conventional endoscopic imaging procedures. Since OCT uses a low coherence interferometer, relaying images outside the body sets special requirements to the endoscope. Transmission has to be high for the IR-wavelengths, which are commonly used for OCT, and it has to be ensured that the phase information is not lost by the endoscopic imaging. We describe an endoscopic OCT system which combines a specially designed rigid endoscope with a modified all fiber OCT-system to create OCT images with 15 μm resolution.

2. THEORY

When coupling an endoscope to an OCT system additional optics are introduced in one arm of the OCT interferometer, which have to be compensated for in the reference arm of the interferometer. The endoscopy will also introduce additional chromatic dispersions. Dispersion reduces the signal and degrades the axial resolution in the OCT images, which is otherwise given by the coherence length l_c of the light source^{4,5}. The coherence length l_c itself depends on the central wavelength λ_c and the full width at the half maximum (FWHM) $\Delta\lambda$ of the spectrum of the light source:

$$l_c = \frac{2 \cdot \ln(2)}{\pi} \cdot \frac{\lambda_c^2}{\Delta\lambda_{FWHM}} \quad (1)$$

Chromatic dispersion can be described by higher derivatives of the index of refraction. For calculating the degradation of the axial resolution in first order approach the group velocity dispersion (GVD) D_{chrom} is normally used.

$$D_{chrom}(\lambda) = \frac{\lambda}{c} \cdot \frac{d^2 n_p}{d\lambda^2} \quad (2)$$

where n_p is the phase index of refraction of the optical components, c is the speed of light and λ is the wavelength. Fig. 1 shows the wavelength dependence of the phase and group index of refraction of amorphous quartz on the wavelength and the GVD for quartz and of the optical glass SF57.

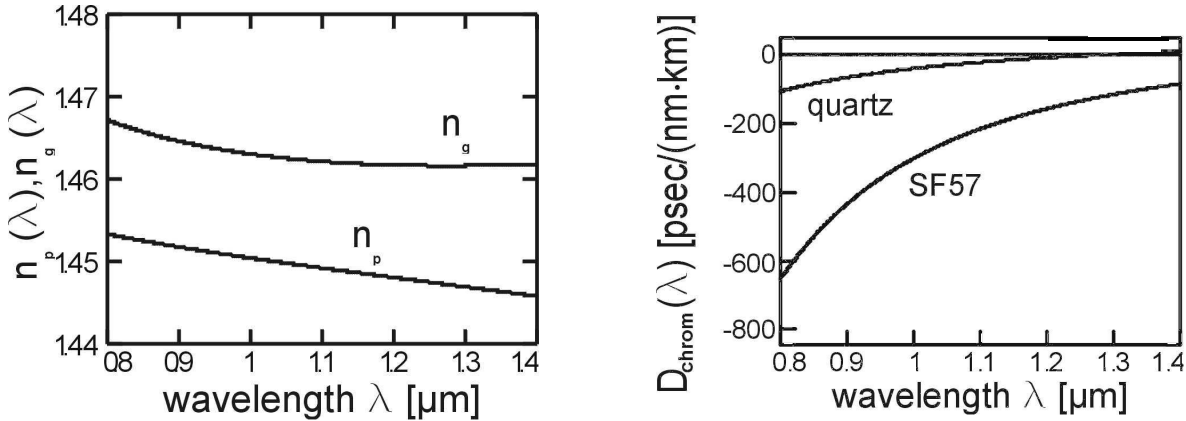


Fig. 1: a) Wavelength dependence of the phase (n_p) and group (n_g) index of refraction of amorphous quartz. b) Wavelength dependence of the GVD of amorphous quartz (single mode fiber core) and of an optical glass SF57.

For quartz the GVD is nearly zero at 1.3 μm . This allows the fabrication of single-mode fibers with zero GVD in this wavelength range. In contrast, glass which is used for manufacturing optical elements usually has a considerable GVD, which leads to a dispersion of the different wavelengths of the OCT spectrum.

Without any optical components the propagation of the electrical field in z direction can be described by equation 3:

$$E_r(z) = \int_{\lambda} P(\lambda) \cdot e^{-i \frac{2\pi}{\lambda} z} d\lambda \quad (3)$$

where $P(\lambda)$ is the power spectrum of the light source and z is the optical path. When an optical element of the thickness d_p is placed in the beam path the phases of the electrical field of the radiation are changed depending on the phase index of refraction n_p and the group index of refraction n_g

$$E_p(z) = \int_{\lambda} P(\lambda) \cdot e^{-i \frac{2\pi}{\lambda} (z + n_p(\lambda) \cdot d_p - n_g(\lambda_c) \cdot d_p)} d\lambda \quad (4)$$

Figure 2 illustrates the effect of the GVD on a pulse (wave packet) with a central wavelength of 800 nm running through 4 mm of SF57-glass. The OCT signal, which is measured by the optical detector, is given by the cross correlation function of electric fields from reference and probe arm. The cross correlation function I without any dispersing material in the interferometer has the width of the coherence length of the light source (Fig. 3a). When 4 mm SF57 is inserted in the sample arm of the OCT interferometer the envelope of the cross-correlation function is broadened (Fig. 3b), and the axial resolution of the OCT is degraded. This can be compensated by introducing similar GVD in the reference arm of the OCT-interferometer, which not necessarily has to be generated by the same material. For example the GVD of 4 mm SF57-glass can be compensated at 800 nm by inserting a 24,73 mm long single mode quartz fiber in the reference arm of the interferometer (Fig. 3c). At this wavelength quartz has a non-zero GVD which is approximately eight times less than that of SF57 (see Fig. 1b).

The width of the cross correlation function (KKB) depends on the central wavelength λ_c , coherence length l_c , spectral width $\Delta\lambda$ of the light source, the GVD D_{chrom} , and the thickness d of the medium. It can be approximated by following equation^{4,5}:

$$KKB(d, D_{\text{chrom}}) = \sqrt{l_c^2 + (D_{\text{chrom}}(\lambda_c) \cdot d \cdot \Delta\lambda)^2} \quad (5)$$

As it was shown in Fig. 2, it is possible to compensate the chromatic dispersion introduced by the endoscope by additional optics in the reference arm of the interferometer. Therefore, for the OCT interferometer two conditions, i. e. similar optical ways defined by the group velocity and similar group velocity dispersions in both arms of the interferometer, have to be fulfilled in order to get optimal resolution and contrast. This can be expressed by following equations:

$$\sum_{i(\text{reference})} n_{g,i} \cdot z_i = \sum_{i(\text{sample})} n_{g,i} \cdot z_i \quad (6)$$

$$\sum_{i(\text{reference})} D_{\text{chrom},i} \cdot z_i = \sum_{i(\text{sample})} D_{\text{chrom},i} \cdot z_i \quad (7)$$

The index i indicates different optical component, $n_{g,i}$ is the group index of refraction, z_i is the length of the optical component, $D_{\text{chrom},i}$ is the group velocity dispersion. By combining standard telecommunication single-mode fibers, which have zero GVD at 1300 nm, with dispersion shifted fibers equations (6) and (7) can easily be fulfilled. This allows to build an all fiber interferometer for an OCT system.

Balancing GVD in both arms of the interferometer is sufficient to achieve an axial resolution of 15 μm . For a higher resolution higher derivatives of n_p by λ have to be considered.

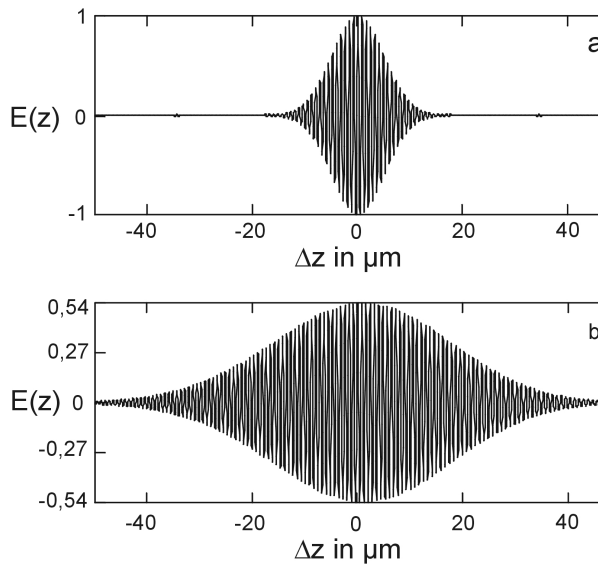


Fig. 2: Simulated wave packet with $\lambda_c=800$ nm, $\Delta\lambda=20$ nm, and $l_c=14,1$ μm traveling in air (a), and traveling through $d=4$ mm SF57 glass (b).

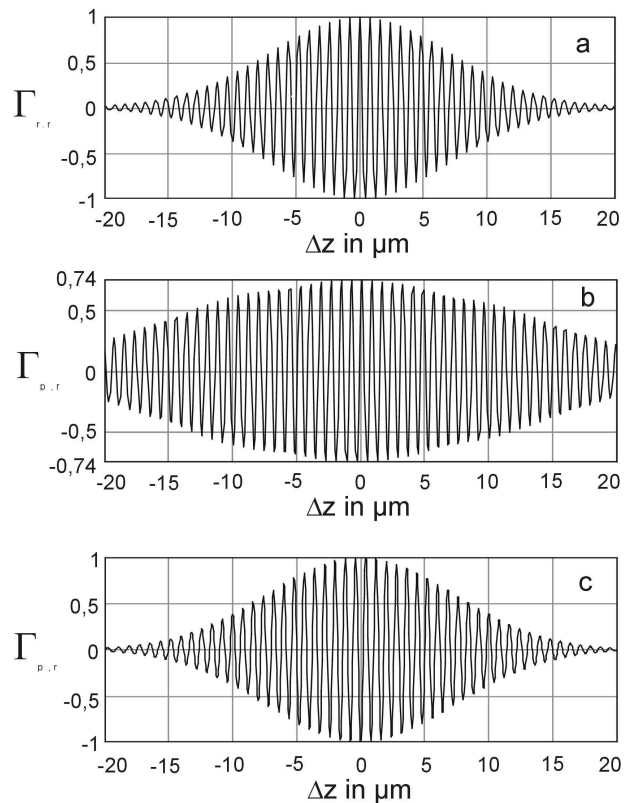


Fig. 3: Calculated cross correlation between probe and reference wave: a) Reference and probe in air. b) Reference traveling in air and probe wave traveling in 4 mm SF57-glass. c) Reference wave traveling through 24,73 mm amorphous quartz (single mode fiber core) and probe wave traveling through $d=4$ mm SF-57-glass.

2.SET-UP FOR RIGID OCT ENDOSCOPE

For endoscopic OCT, a 3 mm rigid endoscope was specially build by the company Richard Wolf GmbH (Knittlingen, Germany). In order to avoid multiple optical surfaces which would need a special AR coating in the visible and at 1300 nm a 270 mm long gradient index lens with specially designed objective (NSG, Temse, Belgium) was used. A 1300 nm OCT system for imaging of skin and the anterior eye chamber (4optics, Luebeck, Germany) was modified for the adaptation to the endoscope. The OCT system consists of an all-fiber interferometer (Corning, Munich, Germany) with fiber stretching for introducing the phase modulation⁵ (Fig. 4). For compensating the additional optical path length and GVD, which is introduced by the endoscope, additional fibers were added to the interferometer. The optical path difference was adjusted by adding an appropriate length z_2 of standard telecom single-mode fiber. A dispersion shifted fiber (LAEF, Corning, Berlin, Germany) with a length of z_1 was used to compensate the GVD. The OCT-system is coupled to the endoscope with a self-build scanner, which focuses the radiation from the mono-mode fiber to the image plane of the gradient index lens. The dielectric scanner mirror transmits visible light so that the top view of the tissue can also be imaged by an endoscopic camera.

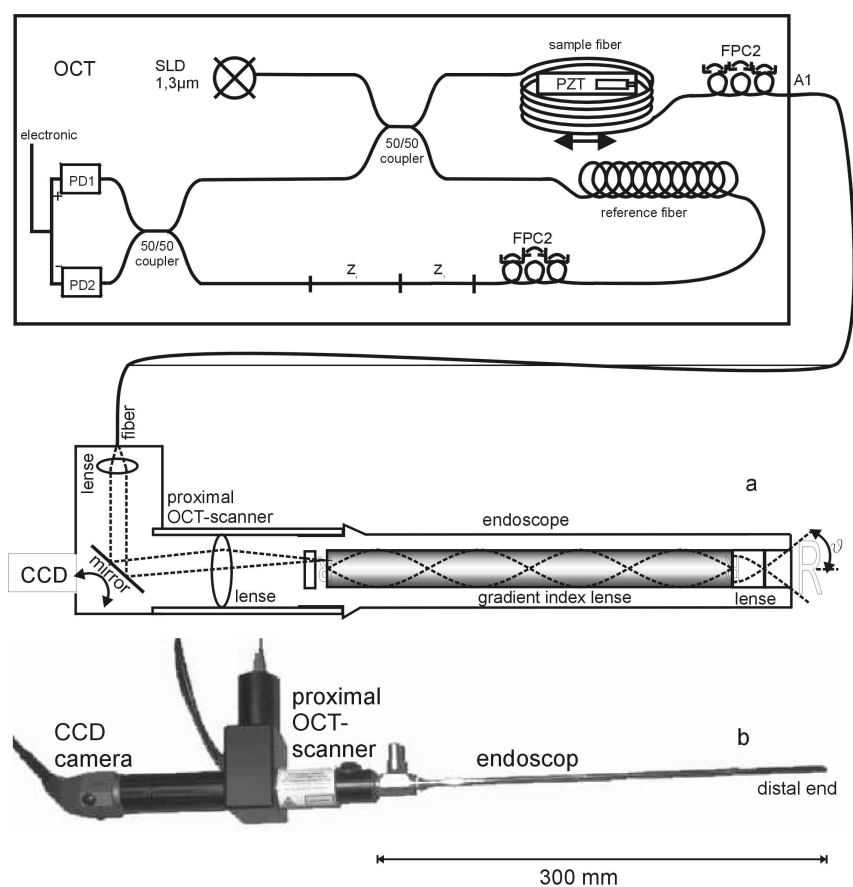


Fig. 4: Rigid OCT endoscope: a) Schematic set-up (SLD = superluminescent diode, z_1 = dispersion shifted fiber, z_2 = single-mode fiber without group velocity dispersion, FPC = fiber polarization controller, pd = photo diode). b) Image of the OCT-endoscope

Since the exact amount of GVD introduced by the endoscope was unknown, the lengths of the compensating fibers were determined experimentally. The axial OCT resolution of the OCT endoscope was measured for different length z_1 of the dispersion-shifted fiber (Fig. 5). A resolution of 15 μm , which was only limited by the coherence length of the SLD, was observed for a fiber length of 1120 mm. Balancing of the GVD in both arms of the interferometer was therefore sufficient to achieve the maximal resolution, which was possible with the superluminescent diode of the OCT system. However when using broader light sources for high resolution OCT also higher order of the chromatic dispersion may have to be compensated.

For a clinical evaluation in the urinary bladder, the safety of the endoscope was certified according to the German law and a permission for clinical tests was obtained.

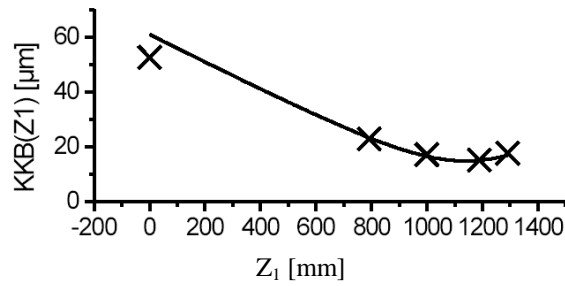


Fig. 5: Width of the cross correlation function (KKB) for different lengths of the dispersion shifted fiber. A mirror in front of the endoscope was used to measure the KKB. The solid line represents according to Eq. 5 expected values for the KKB.

2. EXPERIMENTAL RESULTS

For a first test of the performance of the OCT endoscope, skin was measured with a standard OCT applicator (nearly without chromatic dispersion) and with the OCT endoscope (Fig. 6 and 7). In both images the boundaries between epidermis, dermis and subcutis were visible. The quality was nearly the same.

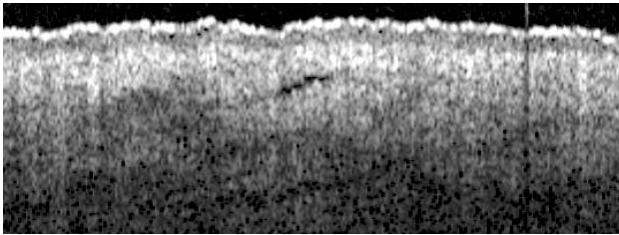


Fig. 6: OCT-image at the upper arm measured without endoscope. (images size: 2.7 mm x 1 mm)

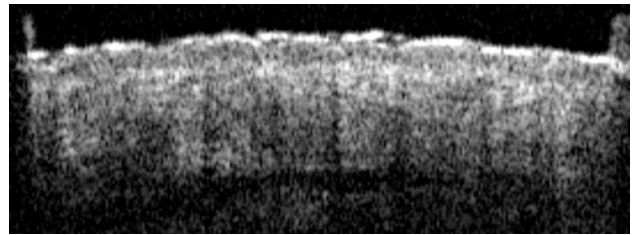


Fig. 7: OCT-image at the upper arm measured with endoscope. (image size: 2,7 mm x 1 mm)

In-vivo images were acquired from different locations of the urinary bladder wall (Fig. 8). Endoscopic OCT could visualize the uppermost tissue layers. The urothelium which is barely light scattering, the lamina propria with a high scattering signal including low scattering blood vessels and the muscle layer could be differentiated in the OCT images.

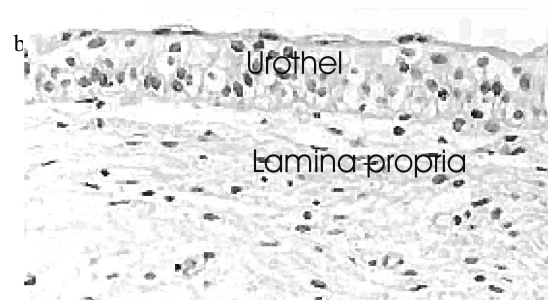
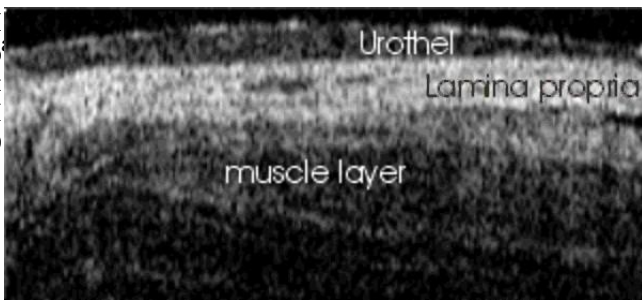


Fig. 8: a) In-vivo OCT image of human bladder wall at $\lambda_c=1,3 \mu\text{m}$ (image size: 1 mm x 2,2 mm). b) Typical histologic image of the uppermost tissue layers of an urinary bladder wall.

Two different OCT system for diagnosis in the urinary bladder, which uses an intracorporal scanner, were reported^{6,7,8}. However up to now, clinical results were obtained only with one system, in which a single-mode fiber is moved in the image plane of objective at the tip of a flexible probe. The bladder wall of more than 60 patients was investigated with similar findings to our preliminary results⁶.

4. CONCLUSION

Altogether we have realized a rigid proximal scanning OCT endoscope with a resolution of about 15 μm . The dispersion compensation of the endoscope is realized by including a dispersion shifted fiber inside the OCT interferometer. Due to the all fiber approach for the OCT interferometer, the instrument is rugged and appropriate for clinical use by non-OCT specialists. Additional to the OCT scan the top view of the tissue, which is investigated, is recorded by a CCD camera. With the newly developed OCT endoscope we can distinguish the uppermost tissue layers of the bladder wall: the urothelium, the lamina propria and the muscle layer. OCT can measure a swelling of the urothelium which is important for diagnosis of precancerous lesions among other things. Endoscopic OCT is an promising additional tool for early bladder cancer diagnosis.

ACKNOWLEDGMENTS

We will thank the Richard Wolf GmbH and 4optics AG for promotion and support of this project.

REFERENCES

1. D. Huang, E. Swanson, C. Lin, J. S. Schuman, W. G. Stinson, W. Chang, M. R. Hee, T. Flotte, K. Gregory, C. A. Puliafito, J. G. Fujimoto, „Optical Coherence Tomography“, *Science*, **254**, 1178-1181 (1991).
2. G. J. Tearney, S. A. Boppart, B. E. Bouma, M. E. Brezinski, N. J. Weissmann, J. F. Southern, J. G. Fujimoto, „Scanning Single-Mode Fiber Catheter-Endoscope for Optical Coherence Tomography“, *Opt. Lett.*, **21**(7), 543-545 (1996).
3. F. König, G. J. Tearney, B. E. Bouma, „Optical Coherence Tomography in Urology“, *Handbook of Optical Coherence Tomography*, Bouma B E, Tearney G J (eds.), 725-737, Marcel Dekker Inc., New York, Basel (2002).
4. C. K. Hitzenberger, W. Drexler, A. Baumgartner, A. F. Fercher, „Dispersion Effects in Partial Coherence Interferometry“, *Coherence Domain Optical Methods in Biomedical Science and Clinical Applications*, Tuchin V V, Podbielska H, Ovaryn B (eds.) SPIE Vol. 2981, 29-36, Proc Soc Photo-Opt Instrum Eng (1997).
5. E. Lankenau, „Optische Kohärenztomographie: Dispersive Einflüsse und Anwendungen in der medizinischen Diagnostik“, Dissertation am Medizinischen Laserzentrum Lübeck, <http://www.dissertation.de> (2003).
6. E.V. Zagaynova, O.S. Streltsova, N.D. Gladkova, L.B. Snopova, G.V. Gelikonov, F.I. Feldchtein, A.N. Morozov, „In Vivo Optical Coherence Tomography Feasibility for Bladder Disease“, *J Urol.*, **167**(3), 1492-1496 (2002).
7. Y.T. Pan, T.Q. Xie, C.W. Du, S. Bastacky, S. Meyers, M.L. Zeidel., „Enhancing Early Bladder Cancer Detection with Fluorescence-Guided Endoscopic Optical Coherence Tomography“, *Opt Lett.* **28**(24), 2485-2487 (2003).
8. T. Xie, H. Xie, G.K. Fedder, Y. Pan, „Endoscopic Optical Coherence Tomography with a Modified Microelectromechanical Systems Mirror for Detection of Bladder Cancers“, *Appl Opt.* **42**(31), 6422-6426 (2003).
9. E. Lankenau, P. Koch, R. Engelhardt, „An Imaging System for Low Coherence Tomography“, In: Trends in Optics and Photonics. Opt Soc Am. OSA, Vol. 2: Advances in Optical Imaging and Photon Migration, 247-249 (1996).
10. E. Lankenau, „Licht ertastet Organe“, *Spektrum der Wissenschaft* No. 07, 92-93 (2002).